supported by the study of Scott et al (Scott et al., 2002) showing that cAMP level was significantly increased and cell number was also increased in a dose-dependent manner in α-MSH using cultured melanocytes with Val92Met compared to those expressing wild-type MC1R. This evidence allows a possible hypothesis that Val92Met caused MC1R to function to proliferate melanoma cells *in vivo* in Japanese.

The well-known active variants, Arg151Cys, Arg160Trp and Asp294His, are strongly believed to be responsible for red hair and fair skin in Caucasian, and the former two in particular were assessed to be involved in melanoma development (van et al., 2001; Matichard et al., 2004). It was no surprise that these three variants, as sources for red hair and fair skin, were not expressed in any of the subjects of this study since none of them had Caucasian characteristics of red hair or fair skin, not even the individuals classified into JST-I. On the contrary, it was notable that none of these active variants, as producers of cutaneous melanoma, was detected in Japanese melanoma cases. We could not definitively explain the essential cause of the difference between Caucasians and Japanese in melanoma development. We could, however, at least speculate that those three active variants in Caucasians are not involved in melanoma development in Japanese, suggesting the possibility that the mechanism of melanoma development could differ innately among ethnic groups. This hypothesis may also explain why SSM is significantly prevalent in Caucasians whereas ALM is the most common form of melanoma in Japanese.

We found other correlations among *MC1R* variants; heterozygous Val92Met

preferred to coexist with heterozygous Arg163Gln and Thr314Thr (A942G), and consensus Val92 was more frequently found with homozygous than heterozygous Arg163Gln, and consensus Thr314 as well (Table III). Other studies have reported the strong linkage between Val92Met and A942G in Caucasians (Bastiaens et al., 2001; Kanetsky et al., 2004) and in a few other populations worldwide (Rana et al., 1999), but no report has noted a similar link between Val92Met and Arg163Gln. Concerning Val92Met, we analyzed statistically the correlation between melanoma and the groups with homozygous or heterozygous Val92Met, heterozygous or consensus Arg163Gln, and homozygous or heterozygous Thr314Thr (A942G), but no statistical significance existed ($p=0.187$). Unlike with Thr314Thr, the series with Val92Met and Arg163Gln is accompanied by the change of amino acids, which may contribute to the stable conformation of proteins, whose role is as active as those provided by the wild-type sequence.

Furthermore, in this study one unexpected but intriguing result was that some allele sequences of blood leukocytes and resected melanoma samples of the same subjects differed from each other (Fig 2). Mutations of other genes such as *BRAF* (Sasaki et al., 2004) in melanoma have been observed and were reported to be associated with the development of tumor. It is not clear yet whether there were biological influences or significance; however, our study may be the first to detect actual alterations of *MC1R* gene in melanoma cells compared with in other somatic cells, indicating that miscellaneous genetic changes occurred in tumor cells and that the variant Val92Met may be susceptible to modification.

In conclusion, we have identified seven variants of *MC1R* gene in the Japanese population, of which Val92Met exhibited a statistical significance in individuals of melanoma cases, especially in non-ALM cutaneous melanoma. Along with some other variants, Val92Met had a tendency to form an alternative combination of DNA sequence. By comparing the *MC1R* sequence of melanoma cells to other somatic cells of the same individual, we observed some differences in the 92nd codon, suggesting genetic alterations in the tumor cells.

ACKNOWLEDGEMENT

We thank Dr. Tomoko Sonoda of Department of Public Health, Sapporo Medical University School of Medicine, for the assistance of statistical analysis. This study was supported in part by Grants-in-Aid from the Ministry of Education, Sports and Culture of Japan, and Ministry of Health, Labour and Welfare of Health and Labour Sciences Research Grants of Research on Advanced Medical Technology.

REFERENCES

Abdel-Malek, Z., Swope, V.B., Suzuki, I., Akcali, C., Harriger, M.D., Boyce, S.T., et al. (1995). Mitogenic and melanogenic stimulation of normal human melanocytes by melanotropic peptides. Proc Natl Acad Sci USA. 92, 1789-1793.

Bastiaens, M.T., ter Huurne, J.A.C., Kielich, C., Kielich, C., Gruis, N.A., Westendorp, R.G.J., et al. (2001). Leiden Skin Cancer Study Team. Melanocortin-1 receptor gene variants determine the risk of nonmelanoma skin cancer independently of fair skin and red hair. Am J Hum Genet. 68, 884-894.

Bohm, M., Luger, T.A. (2000). The role of melanocortins in skin homeostasis. Horm res. 54, 287-293.

Box, N.F., Duffy, D.L., Irving, R.E., Russell, A., Chen, W., Griffiths, L.R., et al. (2001). Melanocortin-1 receptor genotype is a risk factor for basal and squamous cell carcinoma. J Invest Dermatol. 116, 224-229.

Frandberg, P.A., Doufexis, M., Kapas, S., Chhajlani, V. (1998). Human pigmentation phenotype: A point mutation generates nonfunctional MSH receptor. Biochem Biophys Res Commun. 245, 490-492.

Harding, R.M., Healy, E., Ray, A.J., Ellis, N.S., Flanagan, N., Todd, C., et al. (2000). Evidence for variable selective pressures at MC1R. Am J Hum Genet. 66, 1351-1361.

Healy, E., Flannagan, N., Ray, A., Todd, C., Jackson, I.J., Matthews, J.N.S., et al. (2000). Melanocortin-1-receptor gene and sun sensitivity in individuals without red hair. Lancet. 355, 1072-1073.

Hedley, S.J., Gawkrodger, D.J., Weetman, A.P., Morandini, R., Boeynaems, J.M., Ghanem, G., et al. (1998). α-melanocyte stimulating hormone inhibits tumour necrosis factor-□stimulated intercellular adhesion molecule-1 expression in normal cutaneous human melanocytes and in melanoma cell lines. Br J Dermatol. 138, 536-543.

Ichii-Jones, F., Lear, J.T., Heagerty, A.H.M., Smith, A.G., Hutchinson, P.E., Osborne, J., et al. (1998). Susceptibility to melanoma: Influence of skin type and polymorphism in the melanocyte stimulating hormone receptor gene. J Invest Dermatol. 111, 218-21.

Ishihara, K., Saida, T., Yamamoto, A. (2001). The prognosis and statistical investigation committee of the Japanese skin cancer society. Updated statistical data for malignant melanoma in Japan. Int J Clin Oncol. 6, 109-116.

Jimbow, K., Ishida, O., Ito, S., Hori, Y., Witkop, C.J. Jr., King, R.A. (1983). Combined chemical and electron microscopic studies of pheomelanosomes in human red hair. J Invest Dermatol. 81, 506-511.

Jin, H.Y, Yamashita, T., Minamitsuji, Y., Omori, F., Jimbow, K. (2003). Detection of tyrosinase and tyrosinase-related protein 1 sequences from peripheral blood of melanoma patients using reverse transcription-polymerase chain reaction. J Dermatol Sci. 33, 169-176.

Kanetsky, P.A., Ge, F., Najarian, D., Swoyer, J., Panossian, S., Schuchter, L., et al. (2004). Assessment of polymorphic variants in the melanocortin-1 receptor gene with cutaneous pigmentation using an evolutionary approach. Cancer Epidemiol,

Biomarkers Prev. 13, 808-819.

Kennedy, C., ter, Huurne, J., Berkhout, M., Gruis, N., Bastiaens, M., Bergman, W., et al. (2001). Melanocortin 1 Receptor (*MC1R*) gene variants are associated with an increased risk for cutaneous melanoma which is largely independent of skin type and hair color. J Invest Dermatol. 117, 294-300.

Koppula, S.V., Robbins, L.S., Lu, D., Baack, E., White, C.R. Jr., Swanson, N.A., et al. (1997). Identification of common polymorphisms in the coding sequence of the human MSH receptor (MC1R) with possible biological effects. Hum Mutat. 9, 30-36.

Langley, R.G.B., Barnhill, R.L., Mihm, M.C. Jr., Fitzpatrick, T.B., Sober, A.J. (2003). Neoplasms: Cutaneous melanoma. In: Freedberg IM, Eisen AZ, Wolff K, Austen KF, Goldsmith LA, Katz SI, editors. Fitzpatrick's Dermatology in General Medicine, 6th edition. New York: McGraw-Hill. 917-947.

Lens, M.B., Dawes, M. (2004). Global perspectives of contemporary epidemiological trends of cutaneous malignant melanoma. Br J Dermatol. 150, 179-185.

Luger, T.A., Kalden, D., Scholzen, T.E., Brzoska, T. (1999). alpha-melanocyte-stimulating hormone as a mediator of tolerance induction. Pathobiology. 67, 318-321.

Matichard, E., Verpillat, P., Meziani, R., Gerard, B., Descamps, V., Legroux, E., et al. (2004). Melanocortin 1 receptor (*MC1R*) gene variants may increase the risk of melanoma in France independently of clinical risk factors and UV exposure. J Med Genet. 41, e13.

Na, G.Y., Lee, K.H., Kim, M.K., Lee, S.J., Kim, D.W., Kim, J.C. (2003). Polymorphisms in the melanocortin-1 receptor (MC1R) and agouti signaling protein (ASIP) genes in Korean vitiligo patients. Pigment Cell Res. 16, 383-387.

Palmer, J.S., Duffy, D.L., Box, N.F., Aitken, J.F., O'Gorman, L.E., Green, A.C., et al. (2000). Melanocortin-1 receptor polymorphisms and risk of melanoma: Is the association explained solely by pigmentation phenotype? Am J Hum Genet. 66, 176-186.

Park, H.Y., Russakovsky, V., Ao, Y., Fernandez, E., Gilchrest, B.A. (1996). α-melanocyte stimulating hormone-induced pigmentation is blocked by depletion of protein kinase C. Exp Cell Res. 227, 70-79.

Rana, B.K., Hewett-Emmett, D., Jin, L., Chang, B.H.J., Sambuughin, N., Lin, M., et al. (1999). High polymorphism at the human melanocortin 1 receptor locus. Genetics. 151,1547-1557.

Rees, J.L. (2004). The genetics of sun sensitivity in humans. Am J Hum Genet. 75, 739-751.

Ringholm, A., Klovins, J., Rudzish, R., Phillips, S., Rees, J.L., Schioth, H.B. (2004). Pharmacological characterization of loss of function mutations of the human melanocortin 1 receptor that are associated with red hair. J Invest Dermatol. 123, 917-923.

Robinson, S.J., Healy, E. (2002). Human melanocortin 1 receptor (*MC1R*) gene variants alter melanoma cell growth and adhesion to extracellular matrix. Oncogene. 2, 8037-8046.

Sasaki, Y., Niu, C., Makino, R., Kudo, C., Sun, C., Watanabe, H., et al. (2004). *BRAF* point mutations in primary melanoma show different prevalences by subtype. J Invest Dermatol. 123, 177-183.

Satoh, Y., Kawada, A. (1986). Action spectrum for melanin pigmentation to ultraviolet light, and Japanese skin typing. In: Fitzpatrick TB, Wick MM, Toda K, editors. Brown Melanoderma. Biology and Disease of Epidermal Pigmentation. Tokyo: University of Tokyo Press. 87-95.

Schaffer, J.V., Bolognia, J.L. (2001). The melanocortin-1 receptor. Red hair and beyond. Arch Dermatol. 137, 1477-1485.

Schioth, H.B., Phillips, S.R., Rudzish, R., Birch-Machin, M.A., Wikberg, J.E.S., Rees, J.L. (1999). Loss of function mutations of the human melanocortin 1 receptor are common and are associated with red hair. Biochem Biophys Res Commun. 260, 488-491.

Scott, M.C., Wakamatsu, K., Ito, S., Kadekaro, A.L., Kobayashi, N., Groden, J., et al. (2002). Human *melanocortin 1 receptor* variants, receptor function and melanocyte response to UV radiation. J Cell Sci. 115, 2349-2355.

Smith, R., Healy, E., Siddiqui, S., Flanagan, N., Steijlen, P.M., Rosdahl, I., et al. (1998). Melanocortin 1 receptor variants in an Irish population. J Invest Dermatol. 111, 119-122.

Sturm, R.A. (2002). Skin colour and skin cancer – *MC1R*, the genetic link. Melanoma Res. 12, 405-416.

Suzuki, I., Cone, R.D., Im, S., Nordlund, J., Abdel-Malek, Z.A. (1996). Binding of

melanotropic hormones to the melanocortin receptor MC1R on human melanocytes stimulates proliferation and melanogenesis. Endocrinology. 137, 1627-1633.

Tachibana, M. (2000). MITF: A stream flowing for pigment cells. Pigment Cell Res. 13, 230-240.

Thody, A.J., Higgins, E.M., Wakamatsu, K., Ito, S., Burchill, S.A., Marks, J.M. (1991). Pheomelanin as well as eumelanin is present in human epidermis. J Invest Dermatol. 97, 340-344.

Valverde, P., Healy, E., Sikkink, S., Haldane, F., Thody, A.J., Carothers, A., et al. (1996). The Asp84Glu variant of the melanocortin 1 receptor (*MC1R*) is associated with melanoma. Hum Mol Genet. 5, 1663-1666.

van, der, Velden, P.A., Sandkuijl, .L.A., Bergman, W., Pavel, S., van, Mourik, L., Frants, R.R., et al. (2001). Melanocortin-1 receptor variant R151C modifies melanoma risk in Dutch families with melanoma. Am J Hum Genet. 69, 774-779.

Wikonkal, N.M., Brash, D.E. (1999). Ultraviolet radiation induced signature mutations in photocarcinogenesis. J Invest Dermatol Symp Proc. 4. 6-10.

Xu, X., Thornwall, M., Lundin, L.G., Chhajlani, V. (1996). Val92Met variant of the melanocyte stimulating hormone receptor gene. Nat Genet. 14, 384.

Table I. The clinical characteristics of melanoma cases

Subtype	n (%)*	Mean age ± SD	Male	Female	Japanese skin type †	Clinical stage ‡	Tumor thickness (mm)
					I / II / III / NA	0 / I / II / III / IV / NA	
ALM	47 (51.6)	69.2 ± 11.9	19	28	1 / 13 / 3 / 30	2 / 11 / 15 / 10 / 7 / 2	3.2 ± 2.8
SSM	9 (9.9)	47.9 ± 19.4	3	6	1 / 0 / 0 / 8	0 / 4 / 2 / 2 / 1 / 0	1.8 ± 1.7
NM	12 (13.2)	57.5 ± 20.6	6	6	3 / 2 / 1 / 6	0 / 0 / 5 / 7 / 0 / 0	6.0 ± 3.1
LMM	11 (12.1)	62.8 ± 18.8	7	4	1 / 2 / 1 / 7	2 / 2 / 3 / 3 / 1 / 0	4.0 ± 5.5
Others §	12 (13.2)	48.4 ± 18.0	5	7	1 / 5 / 2 / 4	0 / 0 / 2 / 0 / 5 / 5	NS
Unknown	4	50.0 ± 15.4	4	0	1 / 1 / 0 / 2	0 / 0 / 1 / 1 / 1 / 1	NS
Total	95	61.6 ± 17.6	44	51	8 / 23 / 7 / 57	4 / 17 / 28 / 23 / 15 / 8	

ALM, acral lentiginous melanoma; *SSM*, superficial spreading melanoma; *NM*, nodular melanoma, *LMM*, lentigo maligna melanoma; *NA*, data not available; *NS*, data not sufficient

*The percentage shown is the number divided by 91, the total cases not including the four of unknown origin.

† JST-I, burn easily and tan minimally; JST-II, burn moderately and tan moderately; JST-III, burn slightly and tan markedly

‡ Staging was carried out following in the classification of AJCC (2000) according to the individual state when blood was collected.

§ Others included melanomas developing from eye (5), vagina (2), rectum (1) and mucosa (1), or showing histopathologically clear cell sarcoma (1), desmoplastic melanoma (1) and Spitz nevus suspected initially (1).

Table II. The variants of *MC1R* gene in Japanese

Variant	Individual			Haplotype								
				Melanoma (N=95)				Control (N=92)				
	Melanoma (N=95) (%)	Control (N=92) (%)	p-value	C/C*	C/V†	V/V‡	Frequency (%)	C/C*	C/V†	V/V‡	Frequency (%)	p-value
Arg67Gln	4 (4.2)	2 (2.2)	0.683	91	4	0	2.1	90	2	0	1.1	0.433
Ser83Ser (G249A)	0 (0)	1 (1.1)	0.492	95	0	0	0	91	0	1	1.1	0.150
Leu85Gln	1 (1.1)	0 (0)	1.000	94	1	0	0.5	92	0	0	0	0.324
Val92Met	22 (23.2)	11 (12.0)	0.045	73	21	1	12.1	81	9	2	7.1	0.099
Ile120Thr	5 (5.3)	1 (1.1)	0.212	90	5	0	2.6	91	1	0	5.4	0.108
Arg163Gln	94 (98.9)	89 (96.7)	0.297	1	35	59	80.5	3	22	67	84.8	0.277
Thr314Thr (A942G)	20 (21.1)	16 (17.4)	0.526	75	19	1	11.1	74	15	1	9.2	0.611

C, consensus; *V*, variant.

*C/C means the homozygous consensus genotype.

†C/V means the heterozygous genotype.

‡V/V means the homozygous variant genotype.

Table III. The haplotypes of Val92Met and other *MC1R* variants

		Arg163Gln			Thr314Thr (A942G)		
	Val92Met	**C/C***	**C/V†**	**V/V‡**	**C/C***	**C/V†**	**V/V‡**
Melanoma	C/C*	0	15	58	72	1	0
	C/V†	0	20	1	3	18	0
	V/V‡	1	0	0	0	0	1
Control	C/C*	0	14	67	74§	5§	0§
	C/V†	2	7	0	0	9	0
	V/V‡	1	1	0	0	1	1

*C/C means the homozygous consensus genotype.
† C/V means the heterozygous genotype.
‡ V/V means the homozygous variant genotype.
§ Two controls with consensus Val92 could not be analyzed around the area of Thr314 due to fragile response to sequencing.

Table IV. The nonsynonymous variants of *MC1R* gene and melanoma subtypes

Variant	ALM	SSM	NM	LMM	Other	Unknown	Total
Arg67Gln	3 (6.4)				1		4
Leu85Gln		1 (11.1)					1
Val92Met	7 (14.9)	3 (33.3)	4 (33.3)	4 (36.4)	2	2	22
Ile120Thr	3 (6.4)	1 (11.1)					4
Arg163Gln	47 (100)	9 (100)	11 (91.7)	11 (100)	12	4	94
Cases	47	9	12	11	12	4	95

ALM, acral lentiginous melanoma; *SSM*, superficial spreading melanoma; *NM*, nodular melanoma; *LMM*, lentigo maligna melanoma
The parenthetic values are percentage of individuals with variant for cases of each subtype.

FIGURE LEGENDS

Fig 1. Val92Met appeared less frequently in individuals with ALM (7/47, 14.9%) than in those with non-ALM (consisting of SSM, NM and LMM) cutaneous melanoma (11/32, 34.4%).

Fig 2. The cDNA synthesized from blood leukocytes showed homozygous consensus allele of Val92 (left, GenBank: XM047456) whereas genomic DNA collected from paraffin-embedded tissue of metastatic melanoma lesion of the same patient (Case No.51) revealed heterozygous Val92Met (right).

Carcinogenesis vol.27 no.1 pp.53–63, 2006
doi:10.1093/carcin/bgi200
Advance Access publication August 4, 2005

Unique domain functions of p63 isotypes that differentially regulate distinct aspects of epidermal homeostasis

K.E.King, R.M.Ponnamperuma, M.J.Gerdes[1], T.Tokino[2], T.Yamashita[2], C.C.Baker[1] and W.C.Weinberg*

Center for Drug Evaluation and Research, FDA, Bethesda, MD 20892, USA, [1]National Cancer Institute, NIH, Bethesda, MD 20892, USA and [2]Sapporo Medical University School of Medicine, Sapporo 060-8556, Japan

*To whom correspondence should be addressed at: Division of Monoclonal Antibodies, Office of Biotechnology Products, Center for Drug Evaluation and Research, FDA, 29B Lincoln Drive, HFD-123, Building 29B, Room 3NN04, Bethesda, MD 20892-4555, USA. Tel: +1 301 827 0709; Fax: +1 301 827 0852;
Email: weinberg@cber.fda.gov

p63 is critical for squamous development and exists as multiple isotypes of two subclasses, TA and ΔN. ΔNp63 isotypes can antagonize transcription by TAp63 and p53, and are highly expressed in squamous cell cancers. Using mouse keratinocytes as a biological model of squamous epithelium, we show that multiple p63 isotypes, ΔN- and TA-containing, are expressed and differentially modulated during *in vitro* murine keratinocyte differentiation. ΔNp63α declines with Ca^{2+}-induced differentiation, while a smaller ΔN-form, $\Delta Np63_s$, persists, suggesting unique functions of the two ΔN-forms. To investigate the impact of dysregulated p63 expression that is observed in cancers and to define the biological contribution of the different domains of the p63 isotypes, ΔNp63α, $\Delta Np63^{p40}$, TAp63α, TAp63γ or β-galactosidase were overexpressed in primary murine keratinocytes. Microarray, RT–PCR and western blot analyses revealed that overexpression of $\Delta Np63^{p40}$, which lacks the entire α-tail present in ΔNp63α, permits expression of a full panel of differentiation markers. This is in contrast to overexpression of the full-length ΔNp63α, which blocks induction of keratin 10, loricrin and filaggrin. These findings support a role for the α-tail of ΔNp63α in blocking differentiation-specific gene expression. Overexpression of either TAp63 isotype permits keratin 10 and loricrin expression, thus the α-terminus requires the cooperation of the ΔN domain in blocking early differentiation. However, both TA isotypes block filaggrin induction. The ΔN-terminus is sufficient to maintain keratinocytes in a proliferative state, as both ΔN forms block Ca^{2+}-mediated $p21^{WAF1}$ induction and *S*-phase arrest, while sustaining elevated PCNA levels. No alteration in cell cycle regulation was observed in keratinocytes overexpressing TAp63α or TAp63γ. Clarifying the functional distinctions between p63 isotypes and domains will help to elucidate how their dysregulation impacts tumor biology and may suggest novel therapeutic strategies for modulating behavior of tumor cells with altered expression of p53 family members.

Abbreviations: Ad-ΔNp63α, overexpression of ΔNp63α mediated by adenovirus; β-gal, β-galactosidase; BrdU, bromodeoxyuridine; FACS, fluorescence activated cell sorting; MOI, multiplicity of infection.

Introduction

The p53 homologue p63 exists as multiple protein isotypes of two subclasses, TA and ΔN, which arise as a result of alternative promoter usage (1) (Figure 1A). TAp63 isotypes contain a transactivation domain homologous to that of p53 and display overlapping transcriptional activity with p53. In contrast, ΔNp63 isotypes do not contain this domain and are capable of antagonizing transcriptional activity mediated by p53 as well as by TAp63 isotypes (1). Although mutation of *p63* is not common in human cancers, the *p63* gene locus is amplified in squamous cell carcinomas of the head and neck (2–5). Overexpression of p63 protein and mRNA, particularly ΔNp63, has been reported in a variety of squamous cell cancers including those of the head and neck, lung, and skin (5–12). Expression of ΔNp63 isotypes has been associated with undifferentiated cells of proliferative potential in both normal epidermis and tumors (13). We have shown that *in vitro* overexpression of ΔNp63α in primary murine keratinocytes blocks Ca^{2+}-induced growth arrest and differentiation (14). Combined with the expression patterns reported in cancers, this observation suggests a role for ΔNp63α in the maintenance of the basal cell phenotype in normal and neoplastic epithelium.

p63 expression has been reported to progressively increase from the pre-neoplastic lesion to invasive squamous cell carcinoma of the lung (12,15). Reports of TAp63 isotypes in tumors are few, however a trend for decreased TAp63 levels has been correlated with a poor clinical outcome in buccal and laryngeal squamous cell carcinomas (11,16). Co-expression of the ΔN and TAp63 isotypes occurs in normal tissues (17), and in a given cellular context the relative ratios of these isotypes could ultimately affect biological outcome.

Additional variations within the p63 subclasses are the result of C-terminal alternative splicing. α, β and γ variants, which incorporate varying portions of the gene sequence at their C-termini, have been described for both TA and ΔNp63 isotypes (Figure 1A) (18,19). The α-variants are the longest and contain a SAM domain, which is a putative protein–protein interaction domain (20). A second transactivation domain and a transactivation inhibitory domain have been described C-terminal to the SAM domain (21,22). Within the context of the TAp63 subclass, the α-terminus has been reported to auto-inhibit transcriptional activity (22,23). β-Splice variants lack the SAM domain but retain the second transactivation domain, and lose auto-inhibitory activity (22). γ-variants lack the C-terminal exon sequences specific to the α and β variants, but incorporate additional sequences of unknown function from exon 15. The shortest isotype described, $\Delta Np63^{p40}$, is a further ΔN variant that truncates immediately after the oligomerization domain (4).

In this study we used primary murine keratinocytes as a model of squamous epithelium to address the following questions: How is p63 isotype expression altered during normal keratinocyte differentiation? What are the biological roles of

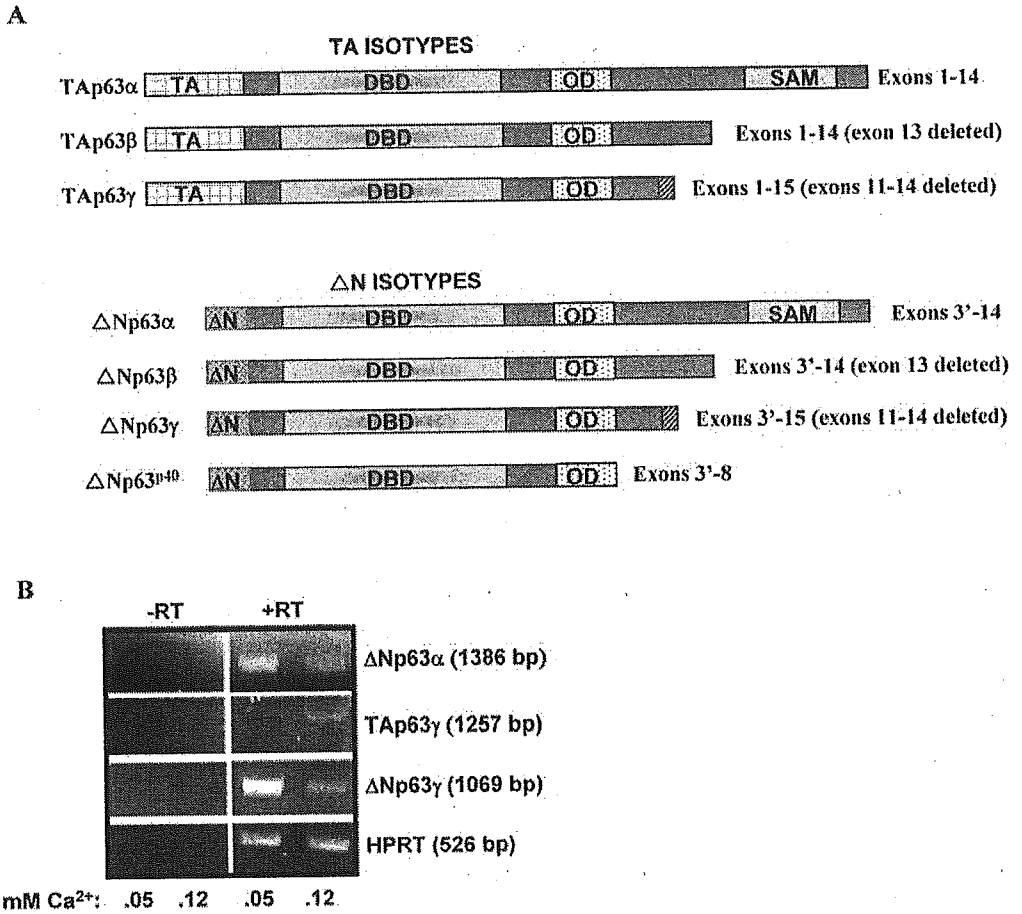

Fig. 1. ΔN and TAp63 isotypes are expressed in primary murine keratinocytes. (A) Graphic depicting the TA and ΔNp63 isotypes. Exon usage is noted next to the isotypes. Exon 3′ is the first exon of ΔNp63 mRNA. Domains noted are: TA, transactivation; DBD, DNA binding; OD, oligomerization; SAM, sterile α-motif. (B) Semi-quantitative RT–PCR analysis of mRNA isolated from proliferating (0.05 mM Ca^{2+}) or differentiating (0.12 mM Ca^{2+}) primary murine keratinocyte cultures 24 h after inducing keratinocyte differentiation via increasing extracellular [Ca^{2+}]. Primers are located within corresponding 5′ and 3′ domains. HPRT is a control for quantitation. Reactions without reverse transcriptase (−RT) were included as negative controls. mRNA expression levels of ΔNp63α and ΔNp63γ decrease with differentiation relative to proliferating cultures, whereas TAp63γ levels increase. No evidence of either TAp63α or TAp63β expression was detected (results not shown). See online Supplementary material for a color version of this figure.

the endogenously expressed forms? What are the specific contributions of the TA and ΔN domains, and how does the C-terminus influence p63 function? To address the latter points, we evaluated the consequences of overexpressing either of two endogenously expressed p63 isotypes (ΔNp63α, TAp63γ), or two C-terminal variants of these isotypes (ΔNp63^{p40}, TAp63α), on keratinocyte proliferation and differentiation. Our findings provide insight into the biological contribution of different functional domains of p63 isotypes and how dysregulation of p63, as observed in squamous cell carcinomas, might contribute to cancer pathogenesis.

Materials and methods

Cell culture

Primary keratinocytes were isolated from the skin of 1–2-day-old C57Bl/6NCr mice and cultured as described previously (24,25). Standard growth medium was composed of Minimal Essential Medium (SMEM) (Life Technologies, Gaithersburg, MD), 8% chelexed fetal bovine serum (FBS) (Gemini BioProducts, Calabasas, CA), 10 U/ml penicillin and 10 ug/ml streptomycin (Life Technologies), at a final concentration of 0.05 mM Ca^{2+}. Differentiation was induced by elevating extracellular [Ca^{2+}] to 0.12 mM (24). Similar patterns of endogenous p63 expression were observed in primary keratinocytes derived from either C57Bl/6NCr or Sencar mice.

Immunostaining

Ethanol-fixed samples of chemically induced mouse skin tumors derived from two-stage carcinogenesis protocols were embedded in paraffin and incubated with peroxidase blocking buffer (KPL, Gaithersburg, MD) followed by pan-p63 antibody (4A4, Santa Cruz Biotechnology, Santa Cruz, CA), or antibodies specific for the ΔN-terminus (p40 Ab-1, Oncogene Research Products, Boston, MA) or α C-terminus (H-129, Santa Cruz Biotechnology). Sections were then incubated with biotinylated secondary antibodies to rabbit or mouse IgG, as appropriate, followed by streptavidin–horseradish peroxidase conjugate, and binding was visualized with Histomark Orange Detection System as per manufacturer's directions (KPL). Nuclei were counterstained with contrast green (KPL).

Adenoviruses and adenoviral infections

Adenovirus encoding ΔNp63α was generated as described previously (14). Adenoviruses encoding TAp63α, TAp63γ, p53 and β-galactosidase (β-gal) were previously described (26) and adenovirus encoding ΔNp63^{p40} (5) was the generous gift of Dr D.Sidransky.

For adenoviral mediated gene transduction, keratinocytes were incubated 60 min at 37°C in serum-free growth medium with an equal MOI of one of the following adenoviral constructs: β-gal, ΔNp63α, TAp63α, TAp63γ, ΔNp63^{p40} or p53. Following the incubation, the medium was aspirated and

replaced with SMEM, described above. Expression was verified by western analysis with an antibody that recognizes the p63 core DNA-binding domain.

Western analysis

Soluble and total cell lysates for western analysis were prepared as described previously (14,27). Optitran nitrocellulose membranes (Schleicher and Schuell, Keene, NH) were probed with antibodies recognizing the following of both mouse and human p63: p63 core DNA binding domain (4A4, Santa Cruz Biotechnology or OP132, Oncogene Research Products); p63 TA, α and γ domains (D20, C-18, H129 and N-18, respectively, Santa Cruz Biotechnology); p63 ΔN domain (p40 Ab-1, Oncogene Research Products); actin (AC-15, Sigma Immuno Chemicals, St Louis, MO); $p21^{WAF1}$ and PCNA (OP79 and NA03, Oncogene Research Products); keratins 1, 10, 14 and filaggrin (BABCO, Richmond, CA). Signal was detected using HRP-linked anti-mouse (1:5000), anti-goat (1:10 000) or anti-rabbit (1:1000) secondary antibody as appropriate and enhanced chemiluminescence (ECL, Amersham Pharmacia Biotech, Piscataway, NJ). Results shown are representative of a minimum of two independent experiments.

Fluorescence activated cell sorting (FACS) analysis

Confluent cultures of primary murine keratinocytes were adenovirally infected with Ad-TAp63α, Ad-TAp63γ, Ad-$\Delta Np63^{p40}$ or Ad-β-gal at 1.5 days post-plating and FACS analysis was performed as described previously (14). Briefly, 17 h post-infection the medium was changed and cells were maintained for 24 h in 0.05 mM or 0.12 mM Ca^{2+}. Cultures were pulsed with 10 μM bromodeoxyuridine (BrdU) for the final 4 h. Cell suspensions were fixed in 70% ethanol for 24 h and incubated with an antibody to BrdU (Becton-Dickinson, San Jose, CA) as per the manufacturer's protocol, then washed and resuspended in phosphate buffered saline containing propidium iodide (5 μg/ml). The cell cycle distribution was analyzed using Cell Quest software on a Becton Dickinson FACSCalibur. A minimum of three replicates were analyzed per condition. Results from each of three independent experiments are presented as the mean percentage of cells in S-phase per condition ± standard deviation.

RNA isolation and semi-quantitative RT–PCR for markers of keratinocyte differentiation

Total RNA was isolated from primary murine keratinocytes using an RNAqueous Kit (Ambion, Austin, TX). Contaminating DNA was removed from 10 μg of total RNA by incubation with 5 U DNase I for 1 h at 37°C in a total volume of 100 μl. The reaction was stopped by incubation with 1 μl of stop solution at 65°C for 10 min and the RNA precipitated with 0.1 vol 3 M NaAc (pH 5.2) and 2.2 vol 100% ethanol. RNA (5 μg) was reverse transcribed according to the instructions provided in the SuperScript First Strand Synthesis System for PCR Kit (Invitrogen Life Technologies, Carlsbad, CA) and included 50 ng each of random hexamers and oligo$(dT)_{12-18}$ primer.

Aliquots (2.5%) of the cDNA pools generated by reverse transcription were used as templates in amplification reactions to detect differentiation-specific gene expression. Target sequences were amplified in a reaction mixture containing 1× reaction buffer (10 mM Tris–HCl (pH 8.3), 50 mM KCl and 1.5 mM $MgCl_2$), 400 μM each dNTP (10 mM mix), 5 U AmpliTaq DNA polymerase (all from Applied Biosystems) and 250 ng each primer. Following a 5 min hot start at 94°C, the reaction profile was as follows: denaturation at 94°C for 45 s; annealing (K10: 58°C, 33 cycles; K1: 58°C, 27 cycles; loricrin: 56°C, 30 cycles; filaggrin: 61°C, 30 cycles and GAPDH: 60°C, 25 cycles) for 45 s; elongation at 72°C for 1 min. The following primer sequences were used, and expected product sizes are noted in parentheses:

Keratin 10: 5′-gaatcgcaaggatgctgaag-3′ and 5′-tctccagtcgggtcttgatg-3′ (338 bp);
Keratin 1: 5′-gcaagaccaagatcaatcccac-3′ and 5′-aaattaaggcggctcagcg-3′ (356 bp);
Loricrin: 5′-tacctggccgtgcaagtaag-3′ and 5′-aacaggatacacctggagcgac-3′ (181 bp);
Filaggrin: 5′-gccaagtccattctggagtc-3′ and 5′-ctactgcctggccttctgag-3′ (306 bp);
GAPDH: 5′-tgttcctacccccaatgtgtc-3′ and 5′- tctcttgctcagtgtccttgc-3′ (352 bp).

To achieve greater accuracy, PCR profiles were initially determined over a range of cycles for each primer pair, so that reactions could be stopped before saturation. All RT–PCRs were performed in duplicate or triplicate and results shown are representative of at least two independent RNA preparations.

Semi-quantitative RT–PCR for p63 isotype expression

RNA was isolated and DNase I treated as described above. Total RNA (0.5 μg) was reverse transcribed with Accuscript Reverse Transcriptase (Stratagene, La Jolla, CA) according to the manufacturer's instructions. The reaction mixture included 0.5 μg oligo$(dT)_{18}$ primer.

Aliquots (5%) of the cDNA pools generated by reverse transcription were used as templates in amplification reactions to detect p63 isotype expression. Target sequences were amplified in a reaction mixture that included heat activated Herculase Hotstart DNA polymerase, as per manufacturer's instructions (Stratagene). Following a 3 min hot start at 94°C, reaction profiles were as follows: denaturation at 94°C for 30 s; annealing at 53°C (TAp63γ, ΔNp63γ and TAp63α/β), 54°C (ΔNp63α), or 51°C (HPRT) for 30 s; extension 72°C for 1.5 min. The number of cycles performed for each primer set was: 35 (TAp63γ, ΔNp63α, ΔNp63γ and TAp63α/β) or 25 (HPRT). The α primer recognizes the exon 12–13 splice junction and is therefore specific for the α−terminus. The α/β primer recognizes C-terminal sequences present in exon 12, which are present in both α and β p63 isotypes. Primer sequences were as follows (F: forward; R: reverse):

TA: 5′-ATG TCG CAG AGC ACC CAG-3′ (F)
γ (28): 5′-CTC CAC AAG CTC ATT CCT GAA GC-3′ (R)
ΔN (28): 5′-CCA GAC TCA ATT TAG TGA GCC AC-3′ (F)
α: 5′-ACA ACC TTG CTA AGA AAA CTG A-3′ (R)
α/β (28): 5′-ATT GCG CTG CTG TGG GTT GAT AAG-3′ (R)
HPRT (28): 5′-CGT CGT GAT TAG CGA TGA TGA-3′ (F)
HPRT (28): 5′-TTC AAA TCC AAC AAA GTC TGG C-3′ (R)

All RT–PCRs were performed in duplicate or triplicate and results shown are representative of at least two independent experiments. All experiments included reactions in which RT was omitted as negative controls, and positive size controls derived from amplification reactions using murine p63 isotype cDNA constructs as templates. The identity of PCR products was confirmed by restriction enzyme mapping or nested PCR.

Real-time PCR for quantitation of specific p63 domains

Real-time PCR was performed on RNA samples prepared, DNase I treated and reverse transcribed with Superscript First Strand Synthesis System as for keratinocyte markers, with the exception that 100 ng random hexamers/μg of RNA were utilized. Isoform specific PCR assays were designed so that one primer spanned an exon–exon boundary (29). The exons bridged in each reaction are noted below and the primer that bridges the exon–exon junction is identified by a *.

ΔN (exons 3′ and 4): *5′-cagactcaatttagtgagcc-3′ and 5′-ctgctggtccatgctgtt-3′
α (exons 13 and 14): 5′-cagacttgccaaatcatcc-3′ and *5′-cagcattgtcagtttcttagc-3′
γ (exons 10 and 15): 5′-agatcaaagagtcactggagc-3′ and *5′-caggctgaaaggagatgt t-3′

This approach allows quantification of the ΔN subclass and the specific α and γ splice variants. However, it does not allow direct determination of which subclass, ΔN or TA, the α or γ splice variants belonged.

Levels of 18S RNA were quantified using primers 5′-gccctgtaattggaatgag-3′ and 5′-tatacgctattggagctgga-3′ for the purpose of normalizing efficiency of RT reactions between RNA preparations. Keratin 1 levels were also monitored to provide a positive biological control and confirm suitability of the culture conditions (24), using the following primers: 5′-agctacggtggctcctct-3′ and 5′-ctggtggaaacaaacttcac-3′.

PCR was carried out using the Perkin Elmer SYBR green real-time PCR kit. Reactions and data collection were performed on a Bio-Rad iCycler iQ Real-time PCR Detection System (Bio-Rad, Hercules, CA). Negative controls (TE, mouse genomic DNA, and negative murine cDNA isotype) were included in every assay. A standard curve using the appropriate cloned murine cDNA standard was set up to accompany each reaction to allow for absolute quantification of each isotype. ΔN and α reactions both utilized the same ΔNp63α cDNA standard and a TAp63γ standard was used for the quantification of the γ domain. An additional real-time PCR assay for the DNA binding domain, which is common to these two isotypes, was used to ensure the accuracy of the quantitation of these two standards relative to each other. This allows data for all isotypes to be expressed in terms of fg of the cDNA clone for ΔNp63α. Thus, all data may be directly and quantitatively compared. Two-step PCR was carried out with data collection and analysis during the combined annealing and extension step. Denaturation was at 95°C for 15 s and anneal/extension at 60°C for 1 min. Three separate mRNA preparations were evaluated and each mRNA sample was assayed in triplicate. All data were converted to fg of the ΔNp63α cDNA standard. The 18S data were used to generate a normalization factor, which was set to 1 for the 0.05 mM Ca^{2+} sample. This normalization factor was applied to all isotype data to correct for any differences in the efficiency of the reverse transcriptase step and errors in RNA quantitation.

Microarray

To assess the contribution of the α-tail to ΔNp63α function, cDNA microarray analysis was performed on RNA samples isolated with TRIzol reagent (Life Technologies) from keratinocytes overexpressing Ad-ΔNp63α, Ad-$\Delta Np63^{p40}$ or Ad-β-gal (as a control) cultured under 0.12 mM Ca^{2+} conditions. ΔNp63α

versus $\Delta Np63^{p40}$; $\Delta Np63\alpha$ versus β-gal; $\Delta Np63^{p40}$ versus β-gal sample pairs were analyzed using Cy3 and Cy5 dyes on mouse cDNA arrays custom synthesized at the National Cancer Institute, NIH. To confirm accuracy and to avoid bias owing to Cy3 or Cy5 dye, labeling reactions were performed in reverse for each paired set. Each final dataset contained four independent hybridizations from two separate RNA preparations. Labeling, hybridization and detection were carried out with the Genisphere sub-Micro labeling kit according to manufacturer's instructions (Genisphere, Hatfield, PA). Slides were scanned on an Axon 4000B scanner and PMT voltage levels were adjusted to obtain an equivalent overall intensity for Cy3 and Cy5. Scanned

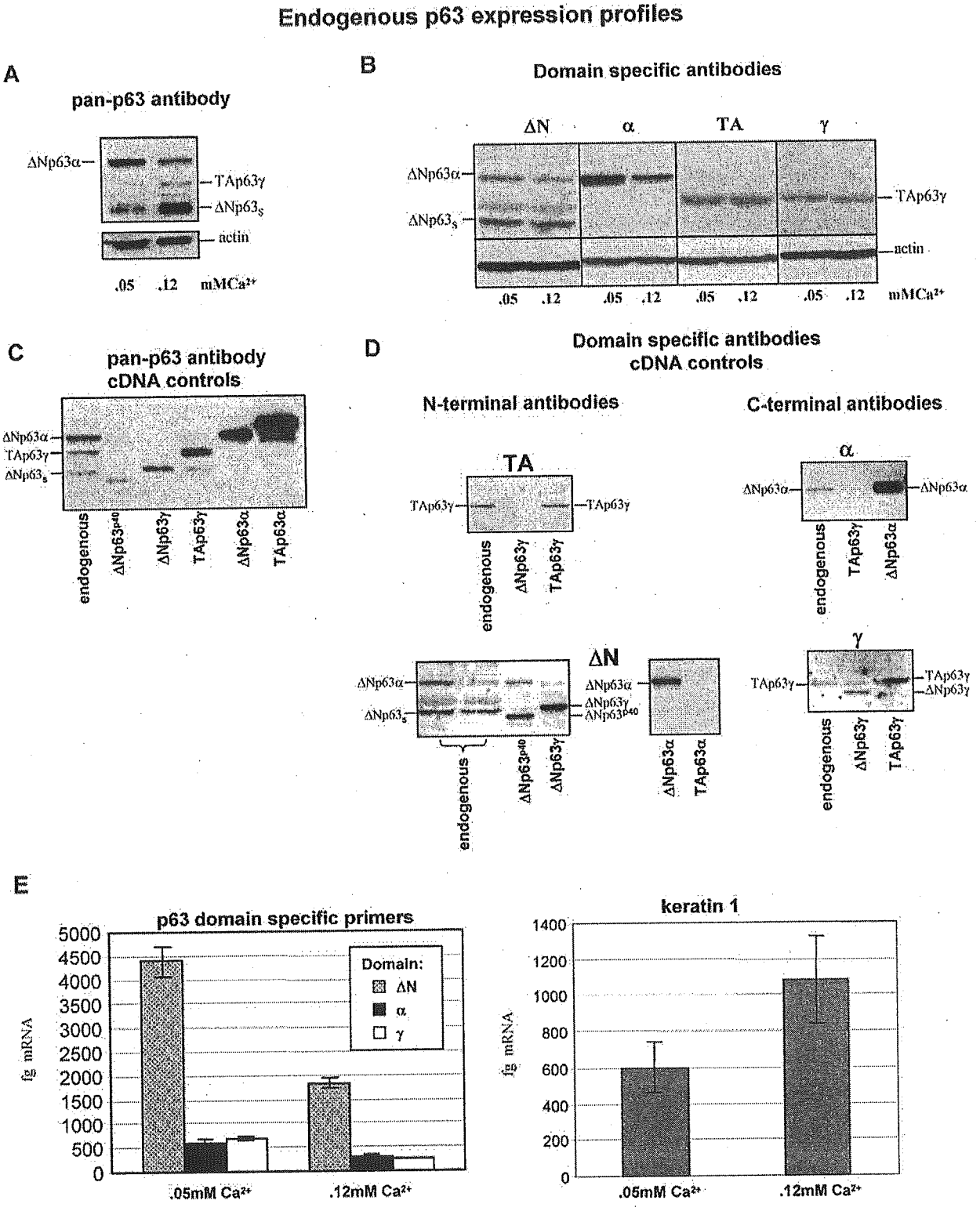

images were then processed with Genepix 4.0 software to quantitate spot intensities for each label. Spots with high artifactual background or no signal were flagged for exclusion. The intensity files were uploaded and analyzed with the mAdb software suite (CIT, NCI, NIH, Bethesda, MD). The following parameters were set for analysis: Target spot size 100–400 μm and 2-fold difference in three of four arrays (75%). Values for the reverse labeling were reciprocated. A table was then generated including the specific spot images with the list of outliers and the respective intensity ratio differences. The spot images were further examined and inadequate spots were excluded. Output was sorted based on ratio values and is presented as mean fold increase.

Results

ΔN and TAp63 isotypes are differentially expressed during keratinocyte differentiation

p63 isotypes can antagonize each other functionally (1) and this modulation may serve to mediate the effects of individual p63 isotypes within both normal and neoplastic environments. Using primary murine keratinocytes as a model of squamous epithelium, we characterized p63 isotype expression patterns at both the mRNA and protein levels in proliferating keratinocyte cultures and after induction of terminal differentiation via the modulation of the extracellular [Ca^{2+}] in the medium from 0.05 to 0.12 mM Ca^{2+} for 24 h.

Semi-quantitative RT–PCR analysis demonstrated readily detectable levels of mRNA for ΔNp63α and ΔNp63γ in proliferating cultures, and very low levels of TAp63γ (Figure 1B). mRNA levels of both ΔNp63 isoforms decline in cultures of differentiating keratinocytes, whereas TAp63γ mRNA levels increase. We found no evidence for expression of mRNA for TAp63α or TAp63β (not shown). The p63 mRNAs observed in these cultures are consistent with those recently reported in intact mouse skin (28). To correlate mRNA and protein levels, we performed western analysis using a pan-p63 antibody that recognizes the core DNA binding domain of p63 as well as domain-specific antibodies directed to either ΔN, TA, α or γ. This revealed a complex pattern of p63 isotype modulation during keratinocyte maturation *in vitro* (Figure 2A). Differential expression and modulation of multiple p63 isotypes was observed following reactivity with a pan-p63 antibody (Figure 2A). The identity of two of these isotypes, ΔNp63α and TAp63γ, was established with the use of domain-specific antibodies (Figure 2B) and confirmed with size standards (Figure 2C). ΔNp63α is the predominant isotype expressed in proliferating keratinocytes and is recognized by the pan-p63 antibody as well as ΔN and α antibodies. The expression pattern observed with all three of these antibodies demonstrates that levels of ΔNp63α decline in maturing keratinocytes (Figure 2A and B, ΔN and α-panels). These results are consistent with the RT–PCR analysis shown in Figure 1 and previous reports (1,13,14,30). In contrast, in multiple independent experiments the level of TAp63γ protein observed in proliferating cultures is sustained or upregulated as keratinocytes differentiate, but never decreases (Figure 2A, pan-p63; Figure 2B, TA and γ-panels). The increase in TAp63γ protein with differentiation correlates with mRNA levels for TAp63γ observed by semi-quantitative RT–PCR (Figure 1B). Controls to confirm the specificity of the domain-specific antibodies are shown in Figure 2D.

A third strong band detected with the pan-p63 antibody and noted in Figure 2A was identified as a member of the ΔN subclass based on an N-terminal specific antibody ($\Delta Np63_s$, Figure 2A and B). Co-migration next to a $\Delta Np63^{p40}$ size standard revealed that this shorter ΔN isotype ($\Delta Np63_s$) migrates between human $\Delta Np63^{p40}$ and murine ΔNp63γ (Figure 2C and D, ΔN antibody). It is not recognized by the γ antibody (Figure 2B), suggesting that it is not ΔNp63γ. Furthermore, the pan-p63 and ΔN western blots did not reveal a species co-migrating with the ΔNp63γ size control (Figure 2C and D). Based on the contrasting results between the RT–PCR and western analyses, it appears that the high levels of ΔNp63γ transcript seen by RT–PCR are not translated in primary murine keratinocytes or that the translated protein is very unstable (Figures 1 and 2), and that the additional ΔN band is unique from ΔNp63γ.

Unlike ΔNp63α, $\Delta Np63_s$ persists or increases following induction of terminal differentiation (Figure 2A and B, ΔN, pan-p63 panels). Its relative size as well as the failure of this band to react with a γ-specific antibody (Figure 2B, γ panel) suggests that it is a novel ΔN form, however we cannot exclude the possibility that it is the previously undescribed murine p40 homologue that could have undergone post-translational modification.

The presence of a ΔN isotype in addition to ΔNp63α is supported by quantitative RT–PCR data (Figure 2E). Real-time PCR primers were designed to measure the absolute amounts of ΔN subclass and α or γ specific splice variants. The amount of mRNA for ΔNp63 is substantially more than that measured for α and γ domains combined, consistent with

Fig. 2. Differential expression of ΔN and TAp63 isotypes during keratinocyte differentiation. Protein levels of specific p63 isotypes are independently regulated during differentiation. (**A** and **B**) Endogenous levels of p63 were evaluated by western analysis of samples prepared from proliferating (0.05 mM Ca^{2+}) or differentiating (0.12 mM Ca^{2+}) keratinocytes 24 h after inducing keratinocyte differentiation via increasing extracellular [Ca^{2+}]. (A) The pan-p63 antibody recognizes sequences within the core p63 DNA binding domain and thus reacts with multiple p63 isotypes. Identities of ΔNp63α and TAp63γ were confirmed by the use of domain-specific antibodies (B) and by co-migration with size standard controls (C). ΔNp63α expression declines during differentiation, while TAp63γ remains stable or is upregulated. An additional ΔN variant ($\Delta Np63_s$) is recognized by the pan-p63 and ΔN antibodies and is stably expressed or increases. The increase seen in $\Delta Np63_s$ levels in panel A may reflect the presence of an additional band in 0.12 mM cultures that is recognized by the pan-p63 but not the ΔN antibody. The lysates used in A and B were derived from independent primary keratinocyte preparations. (C and **D**) cDNA controls as size standards for $\Delta Np63^{p40}$, ΔNp63γ, TAp63γ, ΔNp63α and TAp63α were prepared by transfection or adenoviral transduction of primary murine keratinocytes and probed with a panel of p63 antibodies. Controls are shown next to primary murine keratinocyte lysate prepared from proliferating (C) or differentiating (D) keratinocytes. TAp63γ and ΔNp63α co-migrate with the appropriate size controls. $\Delta Np63_s$ migrates between $\Delta Np63^{p40}$ and ΔNp63γ. (D) A single isotype corresponding to TAp63γ is recognized in the murine keratinocyte lysate by the TA specific antibody, whereas two isotypes are recognized in the primary murine keratinocyte lysate by the ΔN antibody. These isotypes correspond to $\Delta Np63_s$ and ΔNp63α identified on the pan-p63 blot. The middle band observed in the ΔN blot does not co-migrate with any bands recognized by the pan-p63 antibody, and is, therefore, believed to be non-specific. The α-specific antibody detected a single α-isotype (endogenous and control). The γ-specific antibody detects both ΔNp63γ and TAp63γ size controls, but only TAp63γ is detected in the primary murine keratinocyte lysate. (**E**) Real-time RT–PCR analysis performed on mRNA samples prepared from proliferating (0.05 mM Ca^{2+}) or differentiating (0.12 mM Ca^{2+}) keratinocytes 24 h after inducing keratinocyte differentiation via increasing extracellular [Ca^{2+}]. mRNA expression of ΔNp63 and the C-terminal α and γ splice variants decreases with differentiation (left panel). Higher levels of ΔN-domain expression than the combined α- and γ-domains support the existence of a ΔN isotype in addition to ΔNp63α and ΔNp63γ. Results are presented as mean fg amounts of mRNA specific for each domain ± SD. Analysis was performed on three independent RNA preparations in triplicate; graph of representative experiment presented. Keratin 1 mRNA levels were monitored to provide a positive control and confirm suitability of culture conditions (right panel).

expression of an additional ΔN isotype. Overall, mRNA for ΔNp63 declines with keratinocyte differentiation, as do expression levels of both C-terminal splice variants tested, α and γ (Figure 2E). Induction of keratin 1 mRNA confirmed the suitability of the culture conditions (Figure 2E, right panel).

These results demonstrate that several p63 isotypes are co-expressed in keratinocytes, and their balance is altered as keratinocytes differentiate.

ΔNp63 is highly expressed in chemically induced tumors of mouse skin

As shown in Figure 3A, immunohistochemical analysis of chemically induced papillomas of mouse skin using the 4A4 pan-p63 antibody revealed a basilar expression pattern, consistent with previous reports of p63 staining in human squamous cell skin tumors (13,31). Similarly, reactivity of well-differentiated carcinomas with this antibody is localized to keratinocytes removed from areas of differentiation (Figure 3B). α and ΔN domain specific antibodies yielded similar expression patterns to 4A4, consistent with ΔNp63α expression (Figure 3C and D). A more uniform staining pattern throughout the tumor was seen in undifferentiated carcinomas and was similar to all three antibodies (not shown). Only contrast green counterstain was detected in parallel control sections treated identically but without primary antibody (not shown).

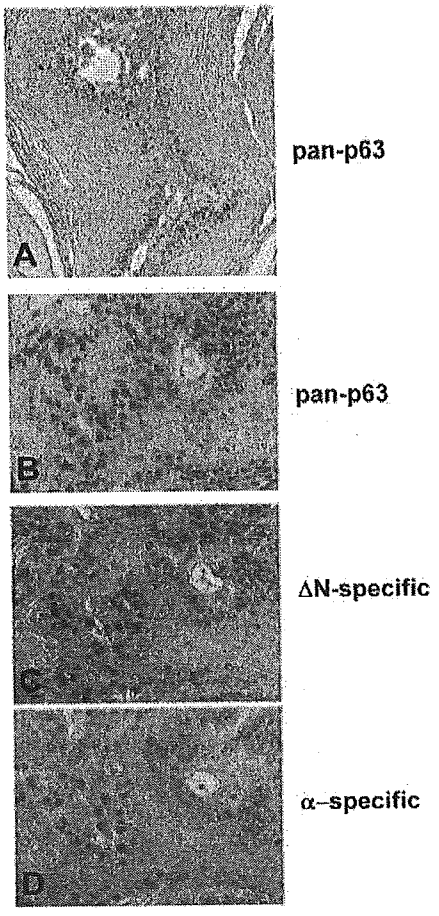

Fig. 3. ΔNp63 is highly expressed in squamous cell tumors. Immunostaining of sections derived from chemically induced tumors of mouse skin. (A and B) Tumor sections incubated with 4A4 pan-p63 antibody show nuclear localization of p63 within basal cells of papillomas (**A**) and in undifferentiated portions of carcinomas (**B**). (**C** and **D**) Neighboring sections of the well-differentiated carcinoma, as shown in B, reacted with ΔN and α specific antibodies. In all cases, p63 staining is localized to keratinocytes removed from centers of differentiation. Results are consistent with high levels of ΔNp63α in these tumors. See online Supplementary material for a color version of this figure.

ΔNp63 isotypes differ in their ability to block keratinocyte differentiation

Previous studies have shown that overexpression of ΔNp63α in keratinocytes prevents the induction of differentiation markers keratin 10 and filaggrin (14). Although the ΔN domain is believed to confer dominant negative properties on this class of isotypes, distinct functions are inferred by the differential expression of full length ΔNp63α and the abbreviated $\Delta Np63_s$ isotype. To elucidate these functional distinctions as well as a potential role of the α-tail, microarray analysis was performed on keratinocytes under differentiating conditions overexpressing either full-length ΔNp63α or $\Delta Np63^{p40}$. At least two sets of direct comparisons were made between the following samples: ΔNp63α versus $\Delta Np63^{p40}$, ΔNp63α versus β-gal and $\Delta Np63^{p40}$ versus β-gal. Strikingly, a number of genes whose expression has been associated with keratinocyte differentiation were noted to be upregulated at least 2-fold in keratinocytes overexpressing $\Delta Np63^{p40}$ relative to ΔNp63α (Table I) (24,32–36), whereas a similar distinction was not observed between keratinocytes overexpressing $\Delta Np63^{p40}$ versus β-gal (data not shown). In contrast, an enhancement of markers associated with basal cells was observed in keratinocytes overexpressing ΔNp63α relative to both $\Delta Np63^{p40}$ and β-gal (Table I) (37–40), consistent with our previous finding that ΔNp63α overexpression blocks keratinocyte differentiation (14). These findings suggested that, in contrast to ΔNp63α (14), overexpression of $\Delta Np63^{p40}$ permits keratinocyte differentiation. This was confirmed by RT–PCR and western analysis of markers of differentiation-specific gene expression (Figures 4A and 5). $\Delta Np63^{p40}$-overexpressing keratinocytes demonstrate normal Ca^{2+}-mediated induction of the full range of differentiation-specific proteins evaluated,

Table I. Microarray analyses of keratinocytes overexpressing $\Delta Np63^{p40}$ or ΔNp63α indicate altered differentiation status of the two populations

Microarray: $\Delta Np63^{p40}$ versus ΔNp63α			
Expression higher in $\Delta Np63^{p40}$		Expression higher in ΔNp63α	
Differentiation associated mRNA (24,32–36)	Mean fold increase	Basal cell associated mRNA (37–40)	Mean fold increase
Filaggrin	2.2	Connexin 26	2.1
Kallikrein 7	4.5	Desmocollin 3	2.4
Claudin 4	2.6	Procollagen XVII α1	2.3
CRABP II	4.1		
Cathepsin L	2.3		

Microarray analysis of mRNA from keratinocytes overexpressing ΔNp63α versus $\Delta Np63^{p40}$ under differentiating (0.12 mM Ca^{2+}) conditions. Data were filtered for enhancement or repression values of 2-fold or greater. Unlike ΔNp63α, $\Delta Np63^{p40}$ allows normal modulation of genes associated with the differentiation response. Keratinocytes overexpressing $\Delta Np63^{p40}$ were also compared with β-gal control keratinocytes, and no significant differences were noted for these genes between the two populations (data not shown).